Received: 30 May 2020 | Revised: 15 October 2020 | Accepted: 3 November 2020

DOI: 10.1111/ejn.15040

RESEARCH REPORT

EJN European Journal of Neuroscience FENS WILEY

Neural generators involved in visual cue processing in children with attention-deficit/hyperactivity disorder (ADHD)

David Zarka[1,2] | **Axelle Leroy**[1] | **Ana Maria Cebolla**[1] | **Carlos Cevallos**[1,3] | **Ernesto Palmero-Soler**[1] | **Guy Cheron**[1,4]

[1]Laboratory of Neurophysiology and Movement Biomechanics, Faculty of Motor Sciences, Université Libre de Bruxelles, Brussels, Belgium

[2]Research Unit in Osteopathy, Faculty of Motor Sciences, Université Libre de Bruxelles, Brussels, Belgium

[3]Departamento de Ingeniería Mecánica, Facultad de Ingeniería Mecánica, Escuela Politécnica Nacional, Quito, Ecuador

[4]Laboratory of Electrophysiology, Université de Mons, Mons, Belgium

Correspondence
Guy Cheron, Laboratory of Neurophysiology and Movement Biomechanics, Faculty of Motor Sciences, Université Libre de Bruxelles, CP640, 808 route de Lennik, 1070 Brussels, Belgium.
Email: gcheron@ulb.ac.be

Funding information
Université Libre de Bruxelles; Secretaria Nacional de Ciencia y Tecnologia; Fonds G. Leibu; NeuroAtt BIOWIN project

Abstract

Event-related potentials (ERP) studies report alterations in the ongoing visuo-attentional processes in children with attention-deficit/hyperactivity disorder (ADHD). We hypothesized that the neural generators progressively recruited after a cue stimulus imply executive-related areas well before engagement in executive processing in children with ADHD compared to typically developed children (TDC). We computed source localization (swLORETA) of the ERP and ERSP evoked by the Cue stimulus during a visual Cue-Go/Nogo paradigm in 15 ADHD compared to 16 TDC. A significant difference in N200/P200 amplitude over the right centro-frontal regions was observed between ADHD and TDC, supported by a stronger contribution of the left visuo-motor coordination area, premotor cortex, and prefrontal cortex in ADHD. In addition, we recorded a greater beta power spectrum in ADHD during the 80–230 ms interval, which was explained by increased activity in occipito-parieto-central areas and lower activity in the left supramarginal gyrus and prefrontal areas in ADHD. Successive analysis of the ERP generators (0–500 ms with successive periods of 50 ms) revealed significant differences beginning at 50 ms, with higher activity in the ventral anterior cingulate cortex, premotor cortex, and fusiform gyrus, and ending at 400–500 ms with higher activity of the dorsolateral prefrontal cortex and lower activity of the posterior cingulate cortex in ADHD compared to TDC. The areas contributing to ERP in ADHD and TDC differ from the early steps of visuo-attentional processing and reveal an overinvestment of the executive networks interfering with the activity of the dorsal attention network in children with ADHD.

KEYWORDS

ADHD, ERP, ERSP, GO/NoGO, N_2, swLORETA

Abbreviations: ADHD, attention-deficit/hyperactivity disorder; BA, brodmann area; DSM, diagnostic and statistical manual of mental disorders; EEG, electroencephalography; ERD, event-related desynchronization; ERP, event-related potential; ERS, event-related synchronization; ERSP, event-related spectral perturbations; ICA, independent component analysis; *SD*, standard deviation; swLORETA, standardized weighted low-resolution electromagnetic tomography; TDC, typically developed children.

Edited by John Foxe

1 | INTRODUCTION

Attention-deficit/hyperactivity disorder (ADHD) is a developmental disorder characterized by age-inappropriate levels of inattention, impulsivity, and hyperactivity that affects about 5% of school-aged children and adolescents (Polanczyk et al., 2015). ADHD implies cognitive and social impairments inducing school difficulties and negative effect on the quality of life (Danckaerts et al., 2010). In the last three decades, interest in the electrophysiological characterization of ADHD through electroencephalography (EEG) has increased in parallel with advances in signal processing (Arns et al., 2016; Lenartowicz & Loo, 2014). In a previous study (Baijot et al., 2017), we used an adapted Go/Nogo paradigm to characterize the time/frequency features related to Cue, Go, and Nogo stimuli in children with ADHD compared to typically developed children (TDC). We highlighted alterations in early P100-N200 components and beta/gamma band (25–45 Hz) event-related desynchronization (ERD) at 300–500 ms in response to visual stimuli (regardless of type: warning, target, or non-target) in children with ADHD compared to TDC. Based on this study, we suggested that ADHD is characterized by a deficit in early visuo-attentional processes, well before engagement in executive processing.

This is supported by numerous event-related potential (ERP) studies reporting alterations in various steps of the ongoing attentional processes in children with ADHD, including smaller frontal selection positivity during visual attentional tasks (Jonkman et al., 2004), atypical P1 features evoked by visual stimuli (Brandeis et al., 2002; Kemner et al., 1996; Perchet et al., 2001; Smith et al., 2004; Steger et al., 2000), alteration of P2/N2 (Banaschewski et al., 2003; Brown et al., 2005; Callaway et al., 1983; Robaey et al., 1992; Satterfield et al., 1994; Senderecka et al., 2012; van Mourik et al., 2007) and reduced P3 (Barry et al., 2006; Brown et al., 2005; Chronaki et al., 2017; Janssen et al., 2016; López et al., 2006; Yorbik et al., 2008) in response to target and non-target stimuli of the oddball task, and attenuated P3 in response to cues from a continuous performance task (Banaschewski et al., 2003; Brandeis et al., 2002; DeFrance et al., 1996; Doehnert et al., 2010; Klorman et al., 1979; Michael et al., 1981; Overtoom et al., 1998; Spronk et al., 2008; Strandburg et al., 1996). These data have generally been interpreted as an early visual filtering deficit, inappropriate attention orienting, impaired stimuli processing, deficient working memory, or deficient resource allocation (Barry et al., 2003; Johnstone et al., 2013).

Event-related studies in the frequency domain have also shown various alterations related to the attentional process in children with ADHD. Namely, delta oscillation was decreased in auditory oddball tasks and visual continuous tasks (Alexander et al., 2008). In others, auditory selective attention task, larger theta (Yordanova et al., 2006) and reduced mu (Yordanova et al., 2013) evoked by irrelevant (non-targets, non-attended) stimuli were reported. The alpha oscillation presented an attenuated event-related desynchronization (ERD) during the encoding phase (Lenartowicz et al., 2014) and an increased occipital power spectrum during the maintenance phase of a spatial working memory task performed by ADHD children (Lenartowicz et al., 2019). In these patients, an increased parieto-occipital gamma band evoked during the encoding phase of a recognition test (Lenz et al., 2008) that did not correlate with performance (Lenz et al., 2008) or differentiate between the known and unknown items (Lenz et al., 2010) was reported. These data suggest an impaired early automatic stimulus classification in ADHD (Lenz et al., 2010) which may involve the cue visual processing into a dysfunctional interaction of the arousal system, including task-irrelevant motor activation (Yordanova et al., 2013) and an impaired memory encoding (Lenartowicz et al., 2014) on a multi-scale large network level (Kim et al., 2015).

In light of these previous studies, we hypothesize that the neural generators progressively recruited after the cue are different between children with ADHD and TDC. More specifically, we previously assumed that cortical areas related to executive processing were more strongly recruited during the cue-evoked processing in ADHD children than TDC. To our knowledge, few studies have previously evaluated the event-related EEG sources in children with ADHD (Bluschke, Gohil et al., 2018; Bluschke, Schuster et al., 2018; Burwell et al., 2019; Chmielewski et al., 2018, 2019; Doehnert et al., 2010; Janssen et al., 2016; Khoshnoud et al., 2018; Leroy et al., 2018), and none of them have specifically focused on the time decomposition during early visual cue processing. Based on our previous work showing the alteration of the P100-N200 components and beta/gamma oscillations (Baijot et al., 2017), we conducted a new exploratory study in order to investigate the source localization of the ERP and the event-related spectral perturbation (ERSP) over time in ADHD.

2 | MATERIALS AND METHODS

2.1 | Participants

Based on the previous data with this task (Baijot et al., 2017), we had estimated that the minimal number of subject to include in the study in order to reach a power equal to 0.80 for a corrected-alpha 0.05 was to 12 in each group (from Baijot et al., 2017, P100-N200 mean amplitude was -5.63 ± 6.11 μV in ADHD, 4.68 ± 4.01 μV in TDC). Thirty-one children aged 8 to 14 years were included in the study: 15 ADHD (12 boys, 11.8 ± 1.8 years) and 16 TDC (10 boys, 11.0 ± 2.3 years) matched for gender and age (Table 1). All of the children were recruited by

TABLE 1 Group comparison for age, estimated IQ, parent-rated ADHD Rating Scale, and Go/Nogo errors per block and reaction time to GO

	Group	*N*	Mean	*SD*	*SE*	*SD*	*t*	*p*
SAMPLE data								
Age	ADHD	15	11.8	1.781	0.46	0.995	29	.328
	TDC	16	11.063	2.294	0.574			
QI Tot.	ADHD	15	102.92	7.149	1.846	−0.807	29	.426
	TDC	16	105.66	11.179	2.795			
ADHD Rating Scale								
IA score	ADHD	15	7.4	1.121	0.289	9.357	29	<.001
	TDC	16	2.125	1.893	0.473			
IA %ile	ADHD	15	96.933	1.87	0.483	4.894	29	<.001
	TDC	16	59	29.933	7.483			
HI score	ADHD	15	5.6	2.72	0.702	5.68	29	<.001
	TDC	16	1.125	1.544	0.386			
HI %ile	ADHD	15	89.733	18.763	4.845	5.006	29	<.001
	TDC	16	45	29.439	7.36			
BEHAVIORAL scores								
OM.	ADHD	15	2.246	1.979	0.511	1.269	29	.215
	TDC	16	1.543	0.969	0.242			
COM.	ADHD	15	5.201	5.383	1.39	2.206	29	.035
	TDC	16	1.826	2.825	0.706			
RT (ms)	ADHD	15	574.24	123.9	30.97	2.061	29	.048
	TDC	16	494.02	88.506	22.85			
CV	ADHD	15	0.075	0.042	0.006	1.251	29	.221
	TDC	16	0.059	0.026	0.011			

Abbreviations: IA, inattentive, HI, hyperactive/impulsive; OM, omissions are incorrect Go, OM, commissions are incorrect Nogo; RT, reaction time; CV, coefficient of variation.

paper announcement or common contact through Hôpital Universitaire des Enfants Reine Fabiola, Human Waves Clinic, association TDA/H Belgique, and specialized school A. Herlin in Brussels, Belgium. Children with ADHD were regularly followed by pediatric neurologists and neuropsychologists. They had been diagnosed according to the Diagnostic and Statistical Manual of Mental Disorders (DSM-V) criteria using the caretaker and child semi-structured interview with help from the Schedule for Affective Disorders and Schizophrenia for School-Age Children (Kaufman et al., 1997) and the Wechsler Intelligence Scale for Children (WISC-IV; Wechsler, 2005). The inclusion criteria for TDC were no previous diagnosis of ADHD and failure to meet DSM-V criteria for ADHD. The children's caretakers were asked to complete questionnaires on demographics and past and present medical information in order to exclude participants presenting with particular medico-psychological antecedents, such as traumatic brain injury or any other neurological psychiatric disease. They also completed in both groups the ADHD Rating Scale (DuPaul et al., 1998) in order to assess inattention and hyperactivity/impulsivity symptoms and confirm ADHD subtype (Table 1). Criteria for exclusion for both groups were mental retardation (IQ < 80), seizure disorder, neurological or psychiatric comorbidity, and sensory deficits or pharmacological treatment (other than methylphenidate) that could interfere with behavioral performances or electrophysiological results. All participants were French native speakers and right-handed. They lived in Brussels and were regularly schooled. Eight children (4 ADHD, 4 TDC) came from the same siblings, and nine other children (4 ADHD, 5 TDC) went to the same school. Among children with ADHD, 5 were predominantly inattentive, 10 were of combined subtype, and none were predominantly hyperactive/impulsive. No TDC reached the threshold corresponding to inattentive or hyperactive/impulsive subtype classification. Children regularly treated by methylphenidate ($n = 6$) stopped their medication 48 hr before the experiments. Informed consent was obtained from all participants and their parents. The experimental design was approved by the Ethics Committee of Center Hospitalier Unuversitaire Brugmann and Hôpital Universitaire des

Enfants Reine Fabiola (Brussels, Belgium), in agreement with CONSORT directives and the Helsinki declaration (World Medical Association, 2013).

2.2 | Setup

Subjects were asked to perform a visually Cue-Go/Nogo task (Baijot et al., 2016). They were comfortably seated in front of a 17-inch computer screen at a distance of 120 cm. The Cue, Go and Nogo stimuli were colored in black and displayed on a white background. Figure 1 illustrates the task sequence. In each trial, a visual target stimulus (50% Go [×] or 50% Nogo [+]) was delivered after the warning stimulus (Cue [■]). A random period ranging from 1 to 2 s separated the warning and the target. Each stimulus was presented for 150 ms. Participants were asked to press a button as quickly as possible after the Go stimulus and to retain/inhibit pushing after the Nogo stimulus. Trials were separated by an interval of 2.5 s (Figure 1). The task was divided into five blocks including 60 trials each, with 300 cue stimuli presented to each participant. Regarding behavioral measures, dependent variables were omissions (no responses to Go), commissions (button press to NoGO), reaction time (RT), and the RT variability (Table 1). The RT variability was calculated with the coefficient of variation (CV) of intra-individual reaction times, a normalized measure of dispersion, defined as the ratio of the standard deviation (σ) to the mean (μ): $CV = \sigma/\mu$. Before and after the task, a resting-state recording (2 min eyes opened and 2 min eyes closed) was performed. Brain activity was recorded by an ASA EEG/ERP system (ANT software, the Netherlands) with 128 Ag/AgCI sintered ring electrodes embedded in an active-shield cap (10–20 system) and shielded co-axial cables. Eye movements were monitored using horizontal and vertical electrooculograms. All electrodes were referred to as the left ear lobe. Impedances were kept below 10 kΩ and checked before each recording. Signals were recorded with a sampling rate of 2048 Hz and a resolution of 16 bits.

2.3 | Processing

Off-line data were treated in EEGLAB software (Brunner et al., 2013; Delorme & Makeig, 2004) and in-house MATLAB-based tools (Cheron et al., 2014). Data were filtered using high-pass (0.1 Hz) and low-pass (47.5 Hz) filters. Defective electrodes (max. 6%) were interpolated. Artifactual portions of data were removed by careful visual inspection before independent component analysis (ICA) of continuous data. Ocular (blinks and saccades) and any other remaining artifacts (i.e., muscular or cardiac) were isolated and rejected by ICA based on topographic features available on the EEGLAB manual. Data epochs were extracted from −0.5 to 1 s centered on Cue onset. Epochs were rejected according to a ±100 μV threshold criterion, and automatic epoch rejection of abnormal spectra (0.1–2 Hz, 50 dB, and 20–45 Hz, 5–100 dB). After data treatment, the number of epochs was 234.55 ± 49.87 (78% of total) for ADHD subjects and 260.00 ± 53.98 (86% of total) for TDC. An EEGLAB study design was used to calculate the average data for all subjects.

2.4 | Analysis

First, ERPs were analyzed in both groups according to our previous work (Baijot et al., 2017), between −200 and 600 ms with respect to cue stimulus in every single electrode on the full scalp array. Event-related spectral perturbations (ERSPs, Delorme & Makeig, 2004) were analyzed within the same time window and according to the classical band decomposition from 4 to 45 Hz: theta (4–6 Hz), alpha (6–15 Hz), beta (15–30 Hz), and gamma (30–45 Hz). The ERP/ERSP scalp map and first source localization were obtained using time interval and frequency ranges for which significant differences in ERP and ERSP were observed between the ADHD and TDC groups: N200/P200 component from 180 to 230 ms, beta event-related synchronization (ERS) between 17 and 23 Hz and from 80 to 220 ms (subdivided into two-time segments: 80–180 ms and 180–220 ms). In a second phase, we

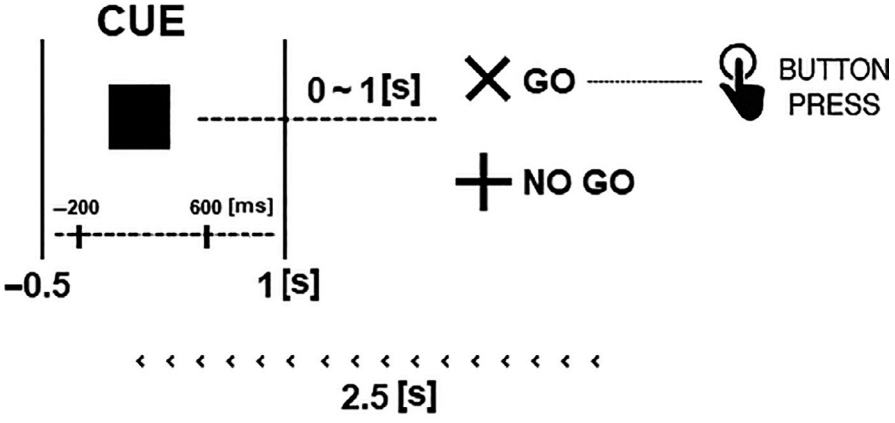

FIGURE 1 Cued Go/Nogo paradigm was adapted from Baijot et al. (2016). The task was divided into five blocks of 60 trials each, with 300 cue stimuli presented to each subject. Data epochs were extracted from −0.5 to 1 s centered on cue onset. The analysis focused on the −200 to 600 ms interval

extended the source reconstruction of ERP from 50 ms to 500 ms. As the interval used to compute N2/P2 source was 50 ms, we performed source analysis in periods of 50 ms around the following selected latencies: 50, 100, 130, 200, 250, 300, 350, 400, 450, and 500 ms in order to explore successive source activation throughout time. This analysis was performed in agreement with the demonstration made by Abeles (Abeles, 2014; Tal & Abeles, 2016) that transients local field potentials related to brief peaks in multiunit activity rates can be approached by the analysis of successive 52 ms slices of data. Such a procedure allows following dynamic variation along time related to interactions between several cortical regions that may not be tightly time-locked to any external cue (Abeles, 2014).

2.4.1 | Time and frequency analysis

For the time domain analysis, ERP was calculated by averaging baseline-corrected epochs extracted from −0.5 to 1 s of the cue onset. The baseline was defined by the time window of 0.5 s before stimulus onset. Post-hoc power analyses were performed with the G*Power 3.1 software (Faul et al., 2009). For time-frequency analysis, we calculated the baseline-normalized spectrogram or ERSP using a fast Fourier transform. ERSP measures variations in the power spectrum of ongoing rhythms at specific periods of time and frequency ranges related to the specific aspect of information processing that is time-locked to the stimulus (Pfurtscheller & Neuper, 1994). In ERSP, ERD (event-related desynchronization) indicates a power spectrum reduction, whereas ERS (event-related synchronization) indicates a power spectrum increase. ERD/ERS is interpreted as reflecting brain reactivity. For this calculation, EEGLAB computes the power spectrum over a sliding latency window and then averages across trials. Each epoch contains samples from −0.5 s before and 1 s after the stimulus. Following the gain model (Delorme & Makeig, 2004), for each frequency band at each frequency point, the power spectrum is divided by the averaged spectral power in the prestimulus baseline period (−0.5 to 0 s). ERSP was calculated with 200 time points, using a window size of 512 samples at 200 linear spaced frequencies from 0.3 to 47.5 Hz. The ERSP image provides a color code at each image pixel, indicating the power reached (in dB) at a given frequency f and latency t relative to the stimulation onset. Typically, for n trials, if $F_k(f, t)$ is the spectral estimate of trial k at frequency f and time t,

$$\mathrm{ERSP}(f,\ t) = \sum_{k=1}^{n} \left| F_k(f,\ t) \right|.$$

To compute $F_k(f, t)$, EEGLAB uses the short-time Fourier transform that provides a specified time and frequency resolution.

2.4.2 | Source analysis

For the source modeling, we performed standardized weighted low-resolution electromagnetic tomography (swLORETA), implemented into ASA Software (ANT Neuro, the Netherlands) (Cebolla et al., 2011, 2017; Leroy et al., 2017; Palmero-Soler et al., 2007). As a distributed inverse solution approach, swLORETA can model spatially distinct sources of neuronal activity from EEG signals without prior knowledge about the anatomical location of the generators. Derived from the sLORETA method (Pascual-Marqui, 2002; Pascual-Marqui et al., 2002; Wagner et al., 2004), swLORETA permits accurate reconstruction of surface and deep current sources, even in the presence of noise and when two dipoles are simultaneously active. This was realized by incorporating a singular value decomposition based lead field weighting that compensated for the varying sensitivity of the sensors to current sources at different depths (Cebolla et al., 2011; Palmero-Soler et al., 2007). The swLORETA solution was obtained using a 3D grid of 2030 points (or voxels) that represented possible sources of the signal. Based on the probabilistic brain tissue maps provided by the Montreal Neurological Institute (MNI) (Collins et al., 1994), the solution was restricted to the gray matter and cerebellum. The 2030 grid points (5.00 mm grid spacing) and recording array (128 electrodes) were indexed by the Collins 27 MRI produced by the MNI (Evans et al., 1993). The Boundary Element Model (BEM) was used to solve the forward problem (Geselowitz, 1967). The final coordinates (x, y, z, Talairach coordinates) were obtained using ASA software and identified as Brodmann areas based on the Talairach atlas (Lancaster et al., 2000).

For the time source analysis of average activity, we first characterized the ERP generators at the previously defined time latency separately for the ADHD and the TDC groups. The current density of every voxel of every participant was divided by the mean current density value of all voxels of the same participant. This gave us a normalized inverse solution in which a voxel value greater than 1 indicates greater activity than the mean. We then calculated the grand average of such normalized inverse solution at a latency of interest for each of the ADHD and TDC groups. To compare group, we created a different image by subtracting the modulus of the swLORETA solution of the ADHD group at the latency of interest to the modulus of the swLORETA solution at the same latency of the TDC group.

Concerning the time-frequency source modeling, the ERSP in brain space over n trials was calculated as proposed by Lin et al. (Lin et al., 2004) as described in detail in Cebolla et al. (Cebolla et al., 2011, 2017): we calculated the brain areas that exhibit ERSP around the previously defined frequency bands of interest. To this end, the analytic signal at the target center frequency was computed for each EEG

sensor channel for the nth trial of the experiment. After that, the swLORETA was applied to the analytic signals for each individual trial. The ERSP in brain space over the n trials were then calculated as (Lin et al., 2004):

$$\mathrm{ERSP}(w,\ t) = \frac{1}{n} + \sum_{n=1}^{n} \mathrm{diag}\left(H_n(w,\ t)\, H_n'(w,\ t)\right),$$

where ERSP(w, t) represents the power spectrum of the swLORETA estimates, n represents the number of trials, diag(M) is a vector formed by the diagonal elements of the matrix M, $H_n(w, t)$ is a row vector containing the analytic signal from the Hilbert transform at time t and frequency w of the swLORETA estimates.

2.5 | Statistics

Differences in ERP and ERSP between groups were determined by the non-parametric permutation test ($n = 800$) and false discovery rate correction provided by the EEGLAB software (Delorme & Makeig, 2004). Considering the number of time points, time-frequency points, and electrodes for ERP, ERSP, and scalp map, respectively, false discovery rate correction was recommended in order to control Type I errors related to the high number of multiple comparisons (Benjamini & Hochberg, 1995; Lindquist & Mejia, 2015). For source analysis, the statistical differences between conditions were determined by the non-parametric permutation method as proposed by Nichols et al. (Nichols & Holmes, 2002) which uses the data itself to generate the probability distribution for testing against the null hypothesis and controls for the false positives that may result from performing multiple hypothesis tests (Nichols & Holmes, 2002). In order to perform the permutation, we use the t test as the value of merit. We compute T-image (T-value per voxel) by performing a one-sample t test (one-tailed) for each voxel of the source space. The null hypothesis is that the distribution of the voxel values of the subjects' difference images has bigger mean in ADHD than TDC (and inversely TDC > ADHD). However, instead of assuming a normal distribution to assess the statistical significance of the T score at each voxel, we used the permutation method to create an empirical distribution as explained in detail by Cebolla et al. (2011). The 95th percentile of the permutation distribution was used for the maximal statistics which defines the 0.05 level of the corrected significance threshold. In other words, we can reject the null hypothesis for any voxel of the un-permuted T image with t-values greater than the 95th percentile of the permutation distribution of the maximal statistics (Holmes et al., 1996).

3 | RESULTS

GO-NoGO scores are summarized in Table 1. The overall means errors during the task were 13,1% (*SD*: ±12,2%) in ADHD and 5,8% (*SD*: ±6.2%) in TDC. ADHD group showed more commission to NoGO [$F(1,29) = 4.87$, $p = .035$] than TDC. No significant difference between groups was found in omission to GO [$F(1,29)$, $p = .215$]. Time reaction was significantly higher in ADHD than TDC [$F(1,29) = 4.25$, $p = .048$] (Figure 2). While ADHD were more variable in their response to GO, we found no significant difference in the reaction time variability between group [$F(1,29) = 1.610$, $p = .221$].

Analysis of ERP evoked by the Cue stimulus at each single channel highlighted group differences obtained in the time domain analysis between −200 and 600 ms. Descriptively, we observed three major occipito-parietal components, namely P100, N200, and P300. Over the centro-frontal region, ERP showed four components: N100, P200, N300, and P400. Figure 2 provided a selection of the ERP waveform superimposition of both groups. The ERP traces exhibited a significantly lower voltage over the centro-frontal regions in ADHD compared to TDC (ADHD: −0.024 ± 1.221 μV, TDC: 2.839 ± 1.217 μV) from 188 ± 11.07 ms to 226 ± 11.20 ms. As illustrated in Figure 3, this difference was characterized by lower P200 amplitude over the frontal region and higher N200 amplitude over the central region (Figure 3a) and was right-lateralized (Figure 3b; corrected $p < .05$, post hoc mean power = 0.77 ± 0.13). Source analysis in both groups revealed that the ERP topography at 200 ms was generated by different generators in each group (Figure 3c). Though the ERP scalp topography of TDC seemed to be explained by the contribution of the bilateral associative visual cortex (BA19: $x = 29.2/-17.1$, $y = -68.7/-80.3$, $z = 42.6/32.0$), the ERP scalp of ADHD patients was characterized by the contribution of the right Broca's pars opercularis (BA44: 54.6, 15.1, 14.5) and fusiform gyrus (BA37: 53.8, −48.0, −14.2). Comparative (ADHD > TDC) analysis of generators highlighted that the left dorsolateral prefrontal cortex (BA46: −42.3, 32.6, 7.7), premotor cortex (BA6: 6.0, 31.2, 34.3), visuo-motor coordination area (BA7: −9.7, −52.6, 68.6), anterior prefrontal cortex (BA10: −13.8, 53.2, 18.4), angular gyrus (BA39: −38.7, −69.1, 16.9), and right superior temporal gyrus (BA22: 46.6, −34.9, 1.3) contributed significantly more to the N200/P200 components in ADHD than in TDC (Figure 3c, left column). The TDC > ADHD contrast did not reveal any significant difference.

ERSP revealed significant differences in the beta band (15–25 Hz) between 80 and 250 ms, with a greater beta power spectrum in ADHD than TDC (Figure 4a; F4: $p = .006$, CP4: $p = .003$). We also noted a significantly

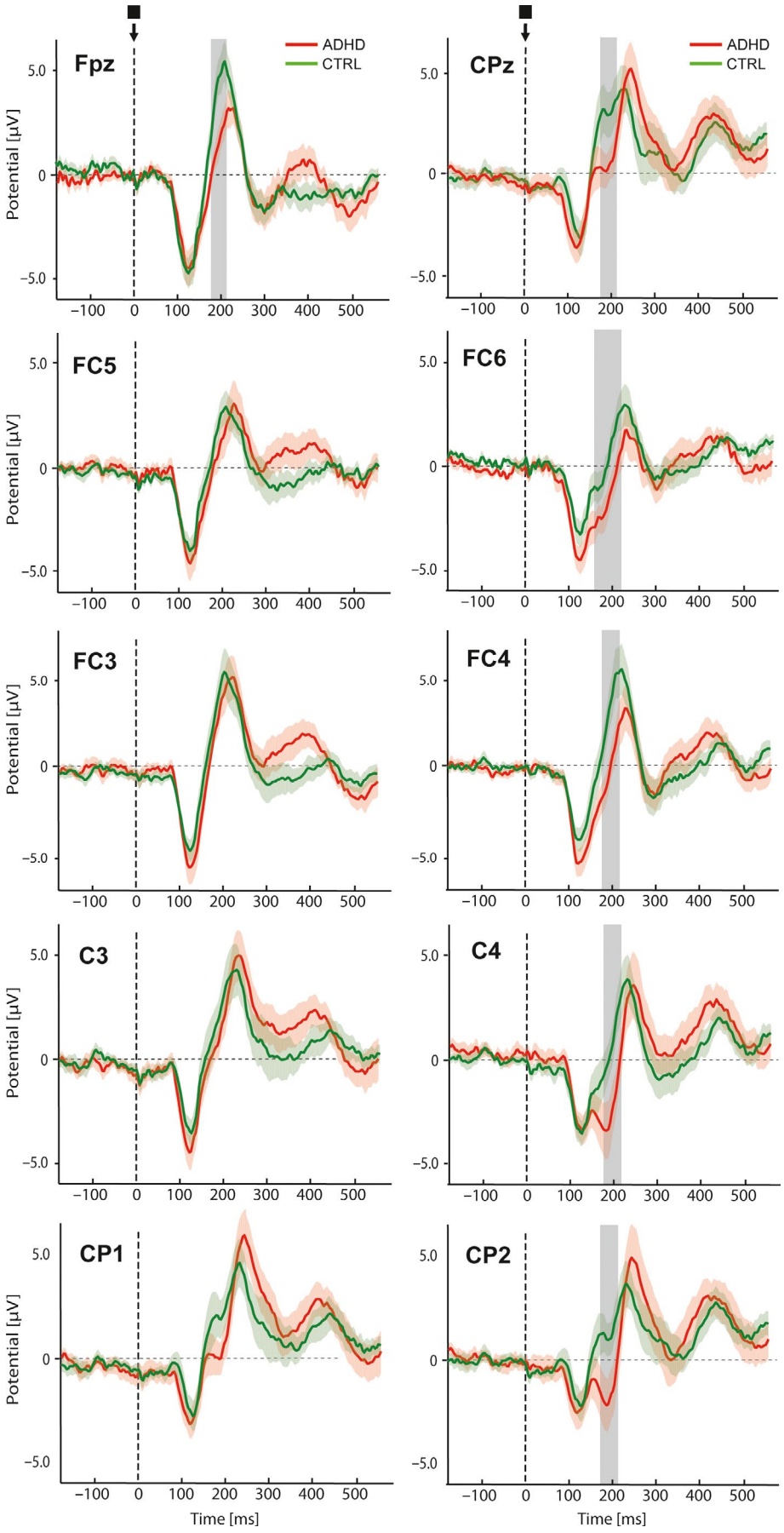

FIGURE 2 Superimposition of the event-related potentials (ERP) evoked by the Cue stimulus in children with ADHD (red) and TDC (green). ERP traces are given with their standard error for both groups. The shaded area indicates a significant group difference ($p < .05$, corrected permutation)

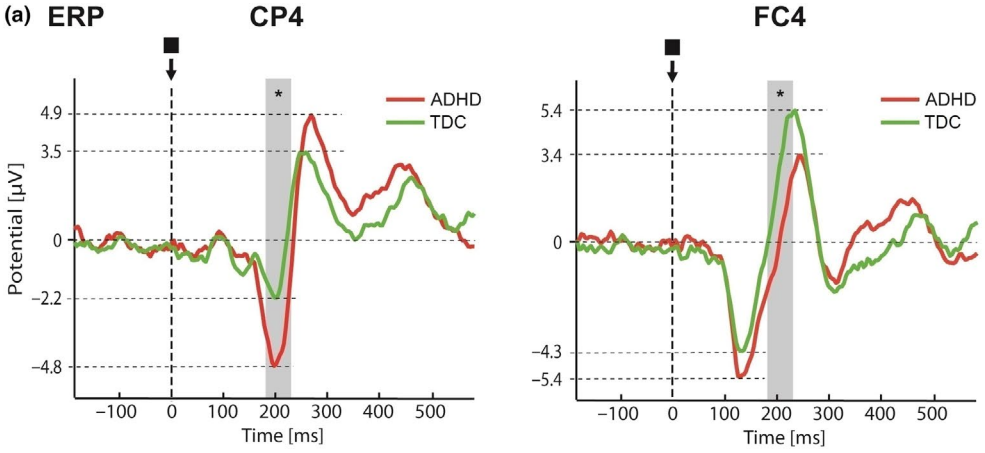
(a) ERP
CP4
FC4
ADHD
TDC
Potential [μV]
4.9
3.5
0
−2.2
−4.8
5.4
3.4
0
−4.3
−5.4
−100 0 100 200 300 400 500
Time [ms]
*

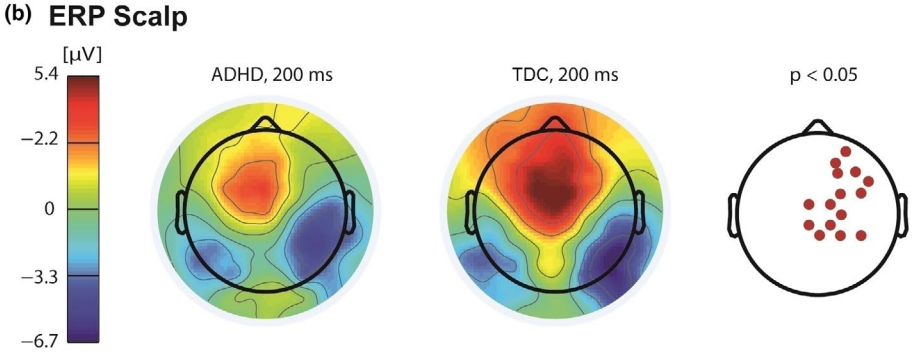
(b) ERP Scalp
[μV]
5.4
−2.2
0
−3.3
−6.7
ADHD, 200 ms
TDC, 200 ms
p < 0.05

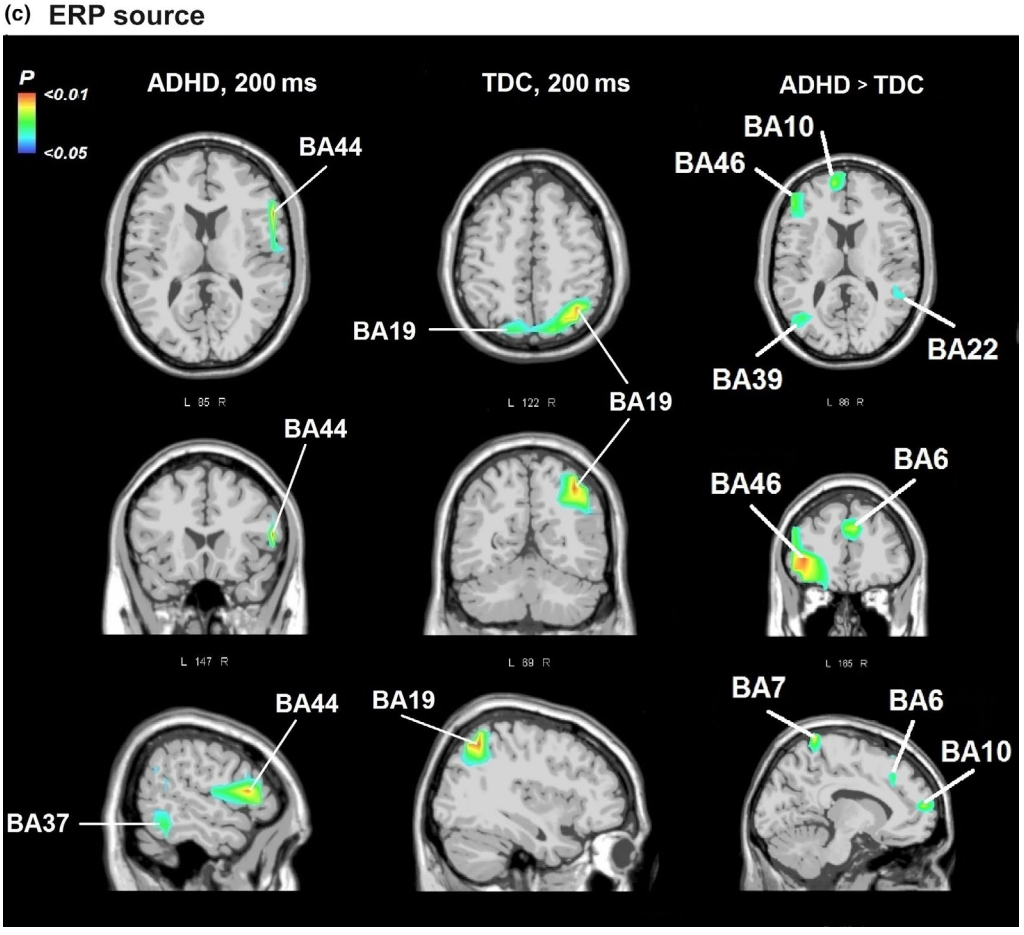
(c) ERP source
P
<0.01
<0.05
ADHD, 200 ms
TDC, 200 ms
ADHD > TDC
BA44
BA19
BA10
BA46
BA22
BA39
BA6
BA7
BA37
L 85 R
L 122 R
L 88 R
L 147 R
L 89 R
L 185 R

FIGURE 3 (a) ERP calculated in the CP4and FC4 electrodes in response to cue stimuli in ADHD and TDC. CP4 mean amplitude on time interval was −2.063 ± 4.70 μV in ADHD and 0.943 ± 3.10 μV in TDC (p = .042). FC4 mean amplitude on time interval was −0.56 ± 3.18 μV in ADHD and TDC = 2.54 ± 4.22 μV (p = .024). N200/P200 time points significance is marked by the gray bar and asterisks ($p < .05$, corrected permutation test). (b) ERP scalp map around 200 ms (50ms interval) in ADHD and TDC. Significant electrodes are marked by a red dot in the third map (corrected permutation test). (c) Source reconstruction at 200 ms (50ms interval) in ADHD and TDC and in contrast ADHD > TDC in the third column. Colors indicate significant areas (corrected permutation test). Note that the TDC > ADHD contrast did not have significant results and is not reported here

lower high-beta/low-gamma (30–35 Hz) power at 400 to 600 ms in ADHD patients compared to TDC (Figure 4a; CP4: p = .013, F4: p = .014). Scalp maps of beta ERS indicated that this difference was marked over the right centro-frontal regions (Figure 4b). Beta power spectrum source analysis (Figure 4c) revealed that the right inferior temporal gyrus (BA20; 45.1, −23.3, −17.7) and fusiform gyrus (BA37; 46.0, −52.1, −16.0), as well as the left associative visual cortex (BA19; −30.4, −77.9, 7.1) were more involved at 130 ms in ADHD than TDC. At approximately 200 ms, these prominent areas in ADHD extended to the angular gyrus (BA39; −47.3, −49.7, 16.9) and the somatosensory association cortex (BA5; −0.5, −31.8, 50.5). In contrast, TDC exhibited a greater contribution of the supramarginal gyrus (BA40; 38.0, −37.4; 30.0) at 130 ms, and the frontal eye fields (BA8; 18.8, 33.5, 44.3) and dorsolateral prefrontal cortex (BA9; 16.0, 53.1, 19.1) at 200 ms.

Source reconstruction sweeping from 50 ms to 500 ms of the ERP (Figure 5) revealed different generators in children with ADHD compared to TDC (ADHD > TDC) along periods. After stimulus onset (50 to 100 ms), swLORETA results indicated a higher contribution of the fusiform gyrus (BA37: 28.1, −43.6, −7.3), and greater activation of the left ventral anterior cingulate cortex (BA24: −0.4/16.7, 14/3.3, 20/29) and left premotor cortex (BA6: −0.8, −20.8, 54.3) in ADHD than TDC. At 130 ms, the somatosensory association cortex (BA5: −19.1, −42.8, 69.5) and visuo-motor coordination area (BA7; 10.3 –61.1, 50.6) increased in ADHD (> TDC). At approximatively 200 and 250 ms following stimulus onset, the left premotor cortex (BA6: −0.8, −20.8, 54.3), dorsal prefrontal cortex of the left side (BA46: −42.3, 32.6, 7.7), anterior prefrontal cortex (BA10; −13.8, 53.2, 18.4) and the angular gyrus of the left side (BA39: −56.1, −58.7, 9.9) contributed more in the ADHD group than TDC. Around 300 and 350 ms, the medial temporal gyrus (BA21: 53.7 7.9 –17.2) and the orbitofrontal area (BA11: 0.7, 36.6, −14.5) of the right side contributed more in the ADHD group with respect to TDC. We also found increased the activation of the associative visual cortex (BA19: 31.1, −57.2, 4.4) and the dorsal anterior cingulate cortex (BA32: 14.9, 30.4, 26.0) at about 350 ms in ADHD. Then, greater involvement of the right dorsolateral prefrontal cortex (BA9: 7.0, 31.2, 34.3) emerged until 450 ms. Finally, activation appeared bilaterally in insula (BA13: −32.0, 23.9, 8.7) at 450 ms, and in the right cerebellar hemisphere (34.5, −31.0, −31.8) at 500 ms. This later cerebellar activity was accompanied by contributions of the left supramarginal gyrus (BA40: −50.3, −50.2, 17.8) and primary visual cortex (BA17: −8.8, −94.2, −4.7).

Statistical reconstruction of the TDC > ADHD contrast did not reveal any difference from the 50 to the 250 ms periods, excepted at 130 ms where the secondary visual cortex (BA18: −8.4, −75.1, −2.4) was activated in TDC > ADHD. At 300 ms, the left motor cortex (BA4: −40.4, −15.0, 38.1) and dorsal cingulate cortex (BA31; −1.3, −39.4, 36.4), and then at 350 ms the left primary somatosensory cortex (BA2: −41.2, −20.3, 28.6) and insula (BA13: −30.5, −12.5, 21.2) were more involved in TDC than in the ADHD group. Finally, at 400 and 450 periods, the ventral and dorsal posterior cingulate cortex (BA23: −0.7, −28.3, 19.3; BA31: −4.4, −70.0, 25.6), as well as the visuo-motor coordination area (BA7: −4.6, −60.6, 41.7), associative visual cortex (BA19: 37.4, −83.8, 7.2; BA18: −7.7, −93.3, 13.7) and bilateral supra marginal gyrus (BA40: 65.0/-50.9, −24.9/-30.8, 18.3/26.7) contributed more in TDC than in the ADHD group.

4 | DISCUSSION

In this study, we explored activity sources involved in the visual cue processing of the Go/Nogo paradigm, which represents the warning stimuli encouraging the participant to focus their attention on the task. In accordance with our hypothesis, we demonstrated that the areas contributing to ERP in ADHD and TDC differ from early steps of visuo-attentional processing revealing altered time sequence processing in the ADHD group. First, our ERP analysis indicated that N200/P200 components evoked by the neutral cue were significantly modified in the absence of any type of final intention (to go or not to go). We observed 54.5% higher parieto-central N200 amplitude and 37.4% lower centro-frontal P200 amplitude in ADHD compared to TDC. Second, we demonstrated that ERP modification at 200 ms over the right centro-frontal regions is accompanied by significant changes in the underlying generators situated in the left premotor cortex (BA46, BA44) and the supplementary motor area (BA6) in children with ADHD. Third, the overtime source identification highlighted a stronger activity of the ventral anterior cingulate cortex (BA24) and fusiform gyrus (BA37) at 50–100 ms,

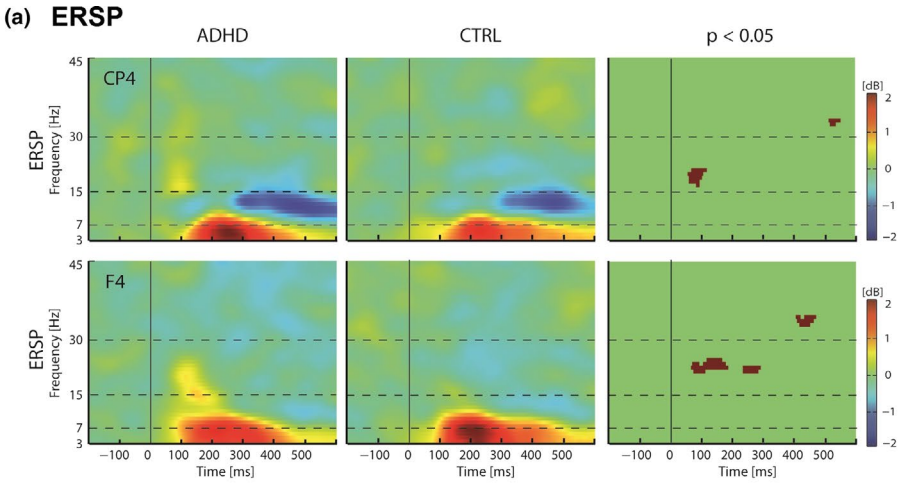
(a) ERSP
ADHD
CTRL
p < 0.05
CP4
F4
ERSP
Frequency [Hz]
45
30
15
7
3
[dB]
2
1
0
−1
−2
−100 0 100 200 300 400 500
Time [ms]

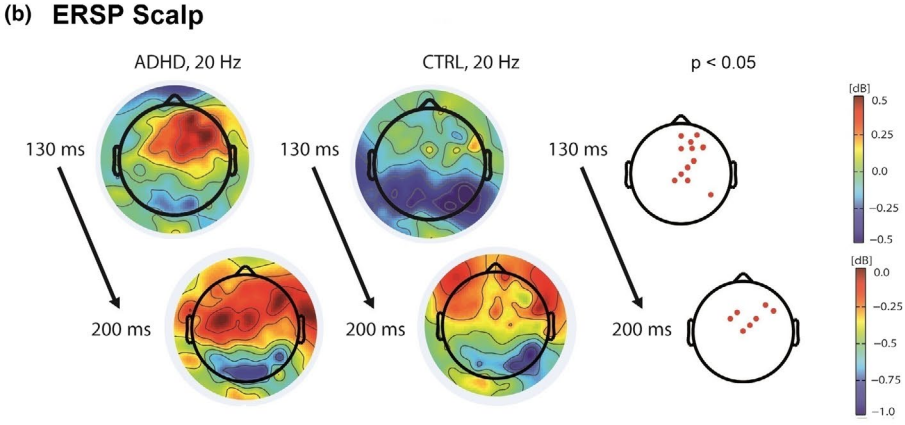
(b) ERSP Scalp
ADHD, 20 Hz
CTRL, 20 Hz
p < 0.05
130 ms
200 ms
[dB]
0.5
0.25
0.0
−0.25
−0.5
0.0
−0.25
−0.5
−0.75
−1.0

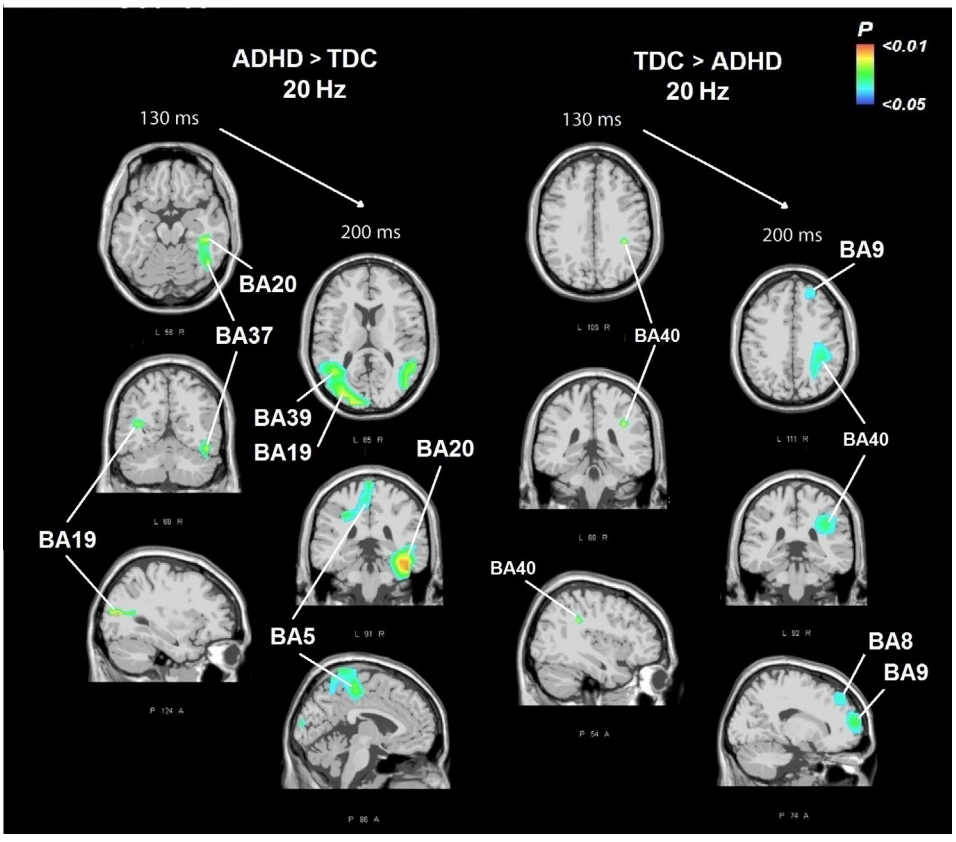
(c) ERSP Source
ADHD > TDC
20 Hz
TDC > ADHD
20 Hz
P
<0.01
<0.05
130 ms
200 ms
BA20
BA37
BA39
BA19
BA5
BA40
BA9
BA8

FIGURE 4 (a) ERSP recorded in the CP4 and FC4 electrodes in response to cue stimuli in ADHD and TDC. Time-frequency significance between groups is highlighted in the third panel (corrected permutation test). (b) 20 Hz scalp map around 130 ms and 200 ms (50 ms interval) in ADHD and TDC. Significant electrodes are marked by a red dot in the third map (corrected permutation test). (c) Source reconstruction of 20 Hz around 130 ms and 200 ms (50 ms interval) in ADHD > TDC and TDC > ADHD contrasts, respectively. Colors indicate significant areas (corrected permutation test)

prolonged by the activation of sensory-motor areas (BA5, BA6, BA7) and the dorsolateral prefrontal cortex (BA9, BA46) in ADHD compared to TDC.

Following the recommendation of Albares et al., (2015), the present methodology combined the use of data processing giving a view on time and time-frequency domains as well as the source of electrophysiological activity. The source analysis using successive 50 ms data slices has previously been introduced in MEG studies (Abeles, 2014; Tal & Abeles, 2016) allowing the identification of the signal dynamics reflecting the short transient local field potentials in the underlying generators. With such procedure, Tal & Abeles (Tal & Abeles, 2016) showed that brief sharp waves of ~20 ms differently distributed over the cortex depending on the different mental tasks can be observed in MEG signals. Few studies (Burwell et al., 2019; Chmielewski et al., 2018, 2019; Doehnert et al., 2010; Janssen et al., 2016; Khoshnoud et al., 2018) have previously evaluated the event-related EEG sources in children with ADHD, but none of them have specifically focused on the time decomposition during early visual processing. Doehnert et al. (2010) and Janssen et al., (2016) focused on the source localization of the P3 alteration related to target stimuli during CPT and the oddball task, respectively, in ADHD compared to TDC. Chmielewski et al. (2018, 2019) investigated source localization related to the modulation of inhibition processes in the Go/Nogo task. Khoshnoud et al. (Khoshnoud et al., 2018) investigated ERP and ERSP independent component clusters during the encoding and reproduction phases of the time reproduction task. Burwell

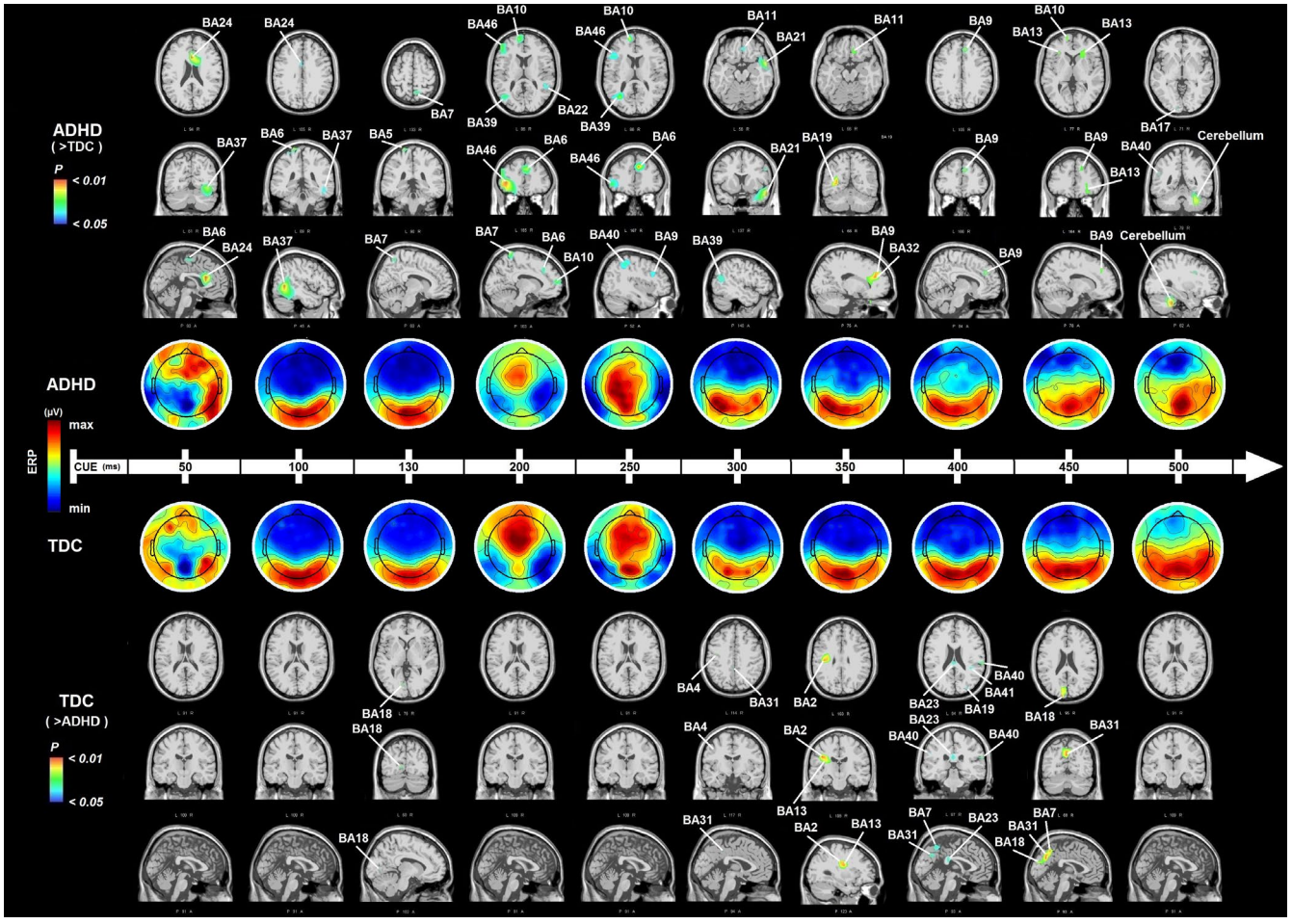

FIGURE 5 Time reconstruction of ERP sources involved from 50 to 500 ms with respect to cue stimuli. Scalp topography show a repartition of potential in time periods of 50 ms around the mentioned latency in ADHD and TDC group separately. Sources were reconstructed in the same time periods and showed ADHD > TDC and TDC > ADHD sources on top and bottom panel, respectively. Colors indicate significant areas (corrected permutation test)

et al. (Burwell et al., 2019) highlighted brain-independent component processes during the error stimuli-response interval of flanker task performance in ADHD.

The present ERP alterations at 150–250 ms corroborated previous studies on attention processing in ADHD (Baijot et al., 2017; Banaschewski et al., 2003; Brown et al., 2005; Buchsbaum & Wender, 1973; Callaway et al., 1983; DeFrance et al., 1996; Lawrence et al., 2005; Lenartowicz et al., 2014; van Mourik et al., 2007; Robaey et al., 1992; Satterfield et al., 1994; Senderecka et al., 2012; Steger et al., 2000). While N200 was long considered as a correlate of inhibition processes, evidence showed that N200 was evoked by a wide variety of paradigm demonstrating that it was also driven by the engagement of high attentional or working memory resources (Albares et al., 2015). In case of ADHD studies, though auditory stimuli evoked generally higher frontal P2 in ADHD than TDC (van Mourik et al., 2007; Satterfield et al., 1994; Senderecka et al., 2012), various visual tasks have been reported to elicit smaller P2 components in the patient group. Specifically, children with ADHD exhibited smaller frontal selection positivity at approximately 200 ms after the stimulus in selective visual tasks compared to control (Jonkman et al., 1997, 2004; van der Stelt et al., 2001), with no differences in later executive or control processes. This was interpreted as an early filtering deficit and explained by posterior-medial dipole alterations (Jonkman et al., 2004). Reduced P2 amplitude in response to a visual non-target stimulus of the oddball task was reported in ADHD children compared to control (Brown et al., 2005), which was interpreted as a general deficit in stimulus registration, facilitation, and processing. More recently, Lenartowicz et al. (Lenartowicz et al., 2014) demonstrated smaller frontal P2 in alerting stimuli preceding the onset of the encoding phase of the working memory task in ADHD compared to TDC, which was related to higher vigilance in the latter group.

Here, the specific contribution of the left premotor cortex (BA46, BA44) and supplementary motor area (SMA, BA6) at about 200 ms suggests an early contribution of the motor network in ADHD, whereas a visual area (BA19) explained the analogous potential topography around 200 ms in TDC that is generally implicated in "what-decision" processing (Adelhöfer et al., 2019). We hypothesized that this motor activation could be related to ADHD impulsivity (Fenollar-Cortés et al., 2017), which could explain the task-irrelevant motor activation (mu rhythm suppression) induced by attended non-target features of stimuli in selective attentional tasks (Yordanova et al., 2013) and corroborate the differential independent mid-frontal sources previously reported between ADHD and TDC at 200–400 ms in a time reproduction task (Khoshnoud et al., 2018). This is yet to be tested, as one of the limitations for the generalization of this study is the absence of the hyperactive ADHD subtype and limited total number of participants.

At the same time, we revealed a significant increase in the centro-frontal beta ERS associated at 130 ms by greater activation of the associative visual cortex (BA19), temporal gyrus (BA20), and fusiform gyrus (B37), and then at 200 ms by greater activation of the associative somatosensory area (BA5) and Wernicke area (BA39) in ADHD compared to TDC. Beta oscillations were generally associated with GABAergic activity and sensorimotor processing (Jensen et al., 2005), but studies demonstrated that beta oscillations were also implicated in cue anticipation and processing and seems reflecting large-scale communication between sensorimotor and other areas (Kilavik et al., 2013). It has been suggested that the increase of beta-band activity could mark deterioration of flexible behavioral and cognitive control (Engel & Fries, 2010). More recently, alpha-beta decrements have been reported as a rhythmic signature of the encoding of working memory in healthy adolescents (Zammit et al., 2018). Taken together, these observations provided converging evidence to an impairment in early cognitive control in ADHD consistent with a compensatory mechanism that tries to alleviate the issues with early attention-related processing, as previously observed during working memory tasks (Lenartowicz et al., 2016). In contrast, contribution of the left supramarginal gyrus (BA40) implicated in visual task selection (Donner et al., 2002), as well as the dorsolateral prefrontal cortex (BA9) and superior and middle prefrontal regions (BA8), suggesting high cognitive evaluation of the cue in TDC. BA8 was recently reported to contribute to the prefrontal P2 component and recognized as a reflection of pre-decision processing in the Go/Nogo task (Adelhöfer et al., 2019), which are effectively present in TDC and absent in ADHD patients. This should indicate that this area is already active at the time of the cue only in TDC.

In the same line of evidence, the stronger activity of the fusiform gyrus (BA37) and ventral anterior cingulate cortex (BA24) at 50–100 ms are in accordance with studies showing that BA37 is involved in visual recognition and BA24 in attention allocation and reward anticipation (Bush et al., 2002; Pardo et al., 1990), and both areas are known to be differentially organized in ADHD (Hoogman et al., 2019; Saad et al., 2017). We also noted a significantly higher contribution of the Wernicke area (BA39) and middle temporal gyrus (BA21) at 200 and 300 ms in children with ADHD compared to TDC. Both of these areas are implicated in the semantic deficit reported in ADHD (Krauel et al., 2009; Mohl et al., 2015; Segal et al., 2015), and their relevant activities here argue in favor of the "short-circuiting" model of ADHD syndrome (Fontenelle & Mendlowicz, 2008). Moreover, middle temporal gyrus (BA21) and the orbitofrontal area (BA11, also active at this latency) have been reported to present lower connectivity in ADHD than controls in the adolescent population (Cabrejo et al., 2019). In addition, an ERP source

study indicated that BA10, BA11, and BA39 are implicated in P3b deficit during an oddball task in ADHD (Janssen et al., 2016). Finally, the late activity of the right lateral cerebellum and left supramarginal gyrus (BA40) implicated in visual task selection (Donner et al., 2002) is in agreement with the right-hand laterality of all of the participants, and corroborated previous studies demonstrating that the cerebellum was recruited differently in ADHD (Bruchhage et al., 2018; Kucyi et al., 2015; Stoodley, 2016). In contrast, TDC did not show specific activity compared to ADHD children until 300 ms. However, TDC showed higher activity of the posterior cingulate cortex (PCC; BA23, BA31) from 300 to 450 ms. These areas are known to be a central node of the default mode network and dorsal attention network (which include insula (Fox et al., 2005) and cerebellum as well (Brissenden et al., 2016)). These both networks are highly related to attention, but show anti-correlated activity. Relative to them, the PCC is hypothesized to play a regulatory role in the balance between internal and external attention, and in arousal (Leech & Sharp, 2014). Studies showed structure and function abnormalities of PCC in ADHD (Castellanos & Proal, 2012; Nakao et al., 2011). In our attentional-demanding context, contributions of PCC, insular, and cerebellum suggested that the dorsal attention network activity began at about 300–350 ms in TDC, and was delayed at about 450 ms in ADHD. Taken together, the overtime analysis of generators seems to suggest an overinvestment of executive networks that interfere with the activity of the dorsal attention network in children with ADHD.

Based on the biological variability encountered in ADHD (gene × environment interactions) the degree to which the present results can be generalized (external validity) (Voelkl et al., 2020) was limited because of the relative small cohorts and complicated by the age range (8 to 15 years old) which encompass the critical transition between childhood and adolescence. Notably, homotypic continuity has been found in childhood depression throughout adolescence (Gaffrey et al., 2018). Stable trajectories of ADHD during this critical period have also been described by O'Neill et al. (O'Neill et al., 2017). In addition, age-related effects primarily impact the strength of the connection instead of their organization (Faghiri et al., 2018), and neural networks involved in sensorimotor and visual processing remain stable from 9 to 25 years of age (Brookes et al., 2018). Although this later MEG study demonstrated an increase in functional connectivity and dynamic stability for alpha and beta oscillations between 9 and 25 years of age, these values are not significantly changed between 9 and 15 years old (Brookes et al., 2018). Another important, and possibly more determinant, factor that should be addressed in detail is the socioeconomic and parental influence during the childhood-adolescence transition (O'Neill et al., 2017). Notably, the fact that some subjects were from sibling pairs could represent a confound factor of our study (Greven et al., 2015). Similarly, although that medication was stopped 48 hr before experiment, regularly methylphenidate treatment of six children with ADHD may interfere in regards to our source localization analysis. The normalization effect of long-term medication on brain structure was a debate in the literature (Hoogman et al., 2017; Nakao et al., 2011). Methylphenidate seems normalize the functional connectivity in ADHD (Rubia et al., 2009). The longitudinal study in rodents confirmed the link between long-term stimulant treatment and striatal hypertrophy (Biezonski et al., 2016), which is recognized as reduced in ADHD (Hoogman et al., 2017). Given the preliminary nature of this study and the heterogeneity of ADHD, its generalization to all ADHD children must be treated with caution. Although, the different types and levels of cognitive dysfunction reported in ADHD (Coghill et al., 2014; Coghill, Seth, Pedroso, et al., 2014) and the present inclusion of 5 inattentive and 10 combined ADHD children, the behavioral score remained homogeneous and not statistically worse than those reported in TDC participants. This limits the possibility that the results may be driven by a subset of participants with one type of ADHD or by a side effect of drowsiness due to medication withdrawal.

ACKNOWLEDGMENTS

We warmly thank the children and their parents who kindly took part in this research. We would also like to thank Anne-Marie Clarinval, M. Petieau, E. Pecoraro T. D'Angelo, E. Toussaint, and E. Hortmans for expert technical assistance. This work was funded by the Université Libre de Bruxelles (Belgium), the Secretaria Nacional de Ciencia y Tecnologia (Senescyt, Ecuador), the Fonds G. Leibu, and the NeuroAtt BIOWIN project supported by the Walloon Region of Belgium.

CONFLICT OF INTEREST

Authors declare no potential sources of conflict of interest.

AUTHOR CONTRIBUTIONS

C.G. and L.A. designed and directed the project, Z.D., L.A., and C.C. performed the experiments, C.G. coordinated recruitment, Z.D and C.C performed data treatment, C.A and P-S. E. provided technical expertize and support, Z.D. and C.G. analyzed results and write the manuscript, C.A proofread the manuscript.

PEER REVIEW

The peer review history for this article is available at https://publons.com/publon/10.1111/ejn.15040.

DATA AVAILABILITY STATEMENT

The detailed table, ERP.avr, and SOURCE.dip files are accessible on fig**share** at the following link: 10.6084/m9.figshare.13089434.

ORCID

David Zarka https://orcid.org/0000-0001-6617-2444
Ana Maria Cebolla https://orcid.org/0000-0002-3710-7923
Carlos Cevallos https://orcid.org/0000-0002-4699-670X
Guy Cheron https://orcid.org/0000-0003-0734-583X

REFERENCES

Abeles, M. (2014). Revealing instances of coordination among multiple cortical areas. *Biological Cybernetics*, *108*, 665–675. https://doi.org/10.1007/s00422-013-0574-2

Adelhöfer, N., Chmielewski, W. X., & Beste, C. (2019). How perceptual ambiguity affects response inhibition processes. *J.*, Neurophysiol. https://doi.org/10.1152/jn.00298.2019

Albares, M., Lio, G., & Boulinguez, P. (2015). Tracking markers of response inhibition in electroencephalographic data: Why should we and how can we go beyond the N_2 component? *Reviews in the Neurosciences*, *26*, 461–478. https://doi.org/10.1515/revneuro-2014-0078

Alexander, D. M., Hermens, D. F., Keage, H. A. D., Clark, C. R., Williams, L. M., Kohn, M. R., Clarke, S. D., Lamb, C., & Gordon, E. (2008). Event-related wave activity in the EEG provides new marker of ADHD. *Clinical Neurophysiology*, *119*, 163–179. https://doi.org/10.1016/j.clinph.2007.09.119

Arns, M., Loo, S. K., Sterman, M. B., Heinrich, H., Kuntsi, J., Asherson, P., Banaschewski, T., & Brandeis, D. (2016). Editorial Perspective: How should child psychologists and psychiatrists interpret FDA device approval? Caveat emptor. *Journal of Child Psychology and Psychiatry*, *57*, 656–658. https://doi.org/10.1111/jcpp.12524

Baijot, S., Cevallos, C., Zarka, D., Leroy, A., Slama, H., Colin, C., Deconinck, N., Dan, B., & Cheron, G. (2017). EEG Dynamics of a Go/Nogo Task in Children with ADHD. *Brain Sciences*, *7*. https://doi.org/10.3390/brainsci7120167

Baijot, S., Slama, H., Söderlund, G., Dan, B., Deltenre, P., Colin, C., & Deconinck, N. (2016). Neuropsychological and neurophysiological benefits from white noise in children with and without ADHD. *Behavioral and Brain Functions*, *12*, 11. https://doi.org/10.1186/s12993-016-0095-y

Banaschewski, T., Brandeis, D., Heinrich, H., Albrecht, B., Brunner, E., & Rothenberger, A. (2003). Association of ADHD and conduct disorder–brain electrical evidence for the existence of a distinct subtype. *Journal of Child Psychology and Psychiatry*, *44*, 356–376. https://doi.org/10.1111/1469-7610.00127

Barry, R. J., Clarke, A. R., McCarthy, R., Selikowitz, M., & Brown, C. R. (2006). Event related potentials in two DSM-IV subtypes of attention-deficit/hyperactivity disorder: An investigation using a combined modality auditory/visual oddball task. R. Oades (Eds.) *Attention-deficit/hyperactivity disorder (AD/HD) and the hyperkinetic syndrome (HKS): Current ideas and ways forward* (pp. 229–247). New York: Nova Science Publishers.

Barry, R. J., Johnstone, S. J., & Clarke, A. R. (2003). A review of electrophysiology in attention-deficit/hyperactivity disorder: II. *Event-related Potentials. Clin Neurophysiol*, *114*, 184–198. https://doi.org/10.1016/S1388-2457(02)00363-2

Benjamini, Y., & Hochberg, Y. (1995). Controlling the false discovery rate: A practical and powerful approach to multiple testing. *Journal of the Royal Statistical Society: Series B (Methodological)*, *57*, 289–300.

Biezonski, D., Shah, R., Krivko, A., Cha, J., Guilfoyle, D. N., Hrabe, J., Gerum, S., Xie, S., Duan, Y., Bansal, R., Leventhal, B. L., Peterson, B. S., Kellendonk, C., & Posner, J. (2016). Longitudinal magnetic resonance imaging reveals striatal hypertrophy in a rat model of long-term stimulant treatment. *Translational Psychiatry*, *6*, e884. https://doi.org/10.1038/tp.2016.158

Bluschke, A., Gohil, K., Petzold, M., Roessner, V., & Beste, C. (2018). Neural mechanisms underlying successful and deficient multi-component behavior in early adolescent ADHD. *NeuroImage Clinical*, *18*, 533–542. https://doi.org/10.1016/j.nicl.2018.02.024

Bluschke, A., Schuster, J., Roessner, V., & Beste, C. (2018). Neurophysiological mechanisms of interval timing dissociate inattentive and combined ADHD subtypes. *Scientific Reports*, *8*, 2033. https://doi.org/10.1038/s41598-018-20484-0

Brandeis, D., Banaschewski, T., Baving, L., Georgiewa, P., Blanz, B., Schmidt, M. H., Warnke, A., Steinhausen, H.-C., Rothenberger, A., & Scheuerpflug, P. (2002). Multicenter P300 brain mapping of impaired attention to cues in hyperkinetic children. *Journal of the American Academy of Child and Adolescent Psychiatry*, *41*, 990–998. https://doi.org/10.1097/00004583-200208000-00018

Brissenden, J. A., Levin, E. J., Osher, D. E., Halko, M. A., & Somers, D. C. (2016). Functional evidence for a cerebellar node of the dorsal attention network. *Journal of Neuroscience*, *36*, 6083–6096. https://doi.org/10.1523/JNEUROSCI.0344-16.2016

Brookes, M. J., Groom, M. J., Liuzzi, L., Hill, R. M., Smith, H. J. F., Briley, P. M., Hall, E. L., Hunt, B. A. E., Gascoyne, L. E., Taylor, M. J., Liddle, P. F., Morris, P. G., Woolrich, M. W., & Liddle, E. B. (2018). Altered temporal stability in dynamic neural networks underlies connectivity changes in neurodevelopment. *NeuroImage*, *174*, 563–575. https://doi.org/10.1016/j.neuroimage.2018.03.008

Brown, C. R., Clarke, A. R., Barry, R. J., McCarthy, R., Selikowitz, M., & Magee, C. (2005). Event-related potentials in attention-deficit/hyperactivity disorder of the predominantly inattentive type: An investigation of EEG-defined subtypes. *International Journal of Psychophysiology*, *58*, 94–107. https://doi.org/10.1016/j.ijpsycho.2005.03.012

Bruchhage, M. M. K., Bucci, M.-P., & Becker, E. B. E. (2018). Cerebellar involvement in autism and ADHD. *Handbook of Clinical Neurology*, *155*, 61–72.

Brunner, C., Delorme, A., & Makeig, S. (2013). Eeglab – An open source Matlab toolbox for electrophysiologicalresearch. *Biomedizinische Technik/Biomedical Engineering*. https://doi.org/10.1515/bmt-2013-4182

Buchsbaum, M., & Wender, P. (1973). Average evoked responses in normal and minimally brain dysfunctioned children treated with amphetamine. *Archives of General Psychiatry*, *29*, 764–770.

Burwell, S. J., Makeig, S., Iacono, W. G., & Malone, S. M. (2019). Reduced premovement positivity during the stimulus-response interval precedes errors: Using single-trial and regression ERPs to understand performance deficits in ADHD. *Psychophysiology*, e13392. https://doi.org/10.1111/psyp.13392

Bush, G., Vogt, B. A., Holmes, J., Dale, A. M., Greve, D., Jenike, M. A., & Rosen, B. R. (2002). Dorsal anterior cingulate cortex: A role in reward-based decision making. *Proceedings of the National Academy of Sciences of the United States of America*, *99*, 523–528. https://doi.org/10.1073/pnas.012470999

Cabrejo, R., Lacadie, C., Brooks, E., Beckett, J., Sun, A., Yang, J., Chuang, C., Eilbott, J., Duncan, C., Steinbacher, D., Alperovich,

M., Ventola, P., Pelphrey, K., Constable, T., & Persing, J. (2019). Understanding the learning disabilities linked to sagittal craniosynostosis. *Journal of Craniofacial Surgery*, *30*, 497–502. https://doi.org/10.1097/SCS.0000000000005194

Callaway, E., Halliday, R., & Naylor, H. (1983). Hyperactive children's event-related potentials fail to support underarousal and maturational-lag theories. *Archives of General Psychiatry*, *40*, 1243–1248.

Castellanos, F. X., & Proal, E. (2012). Large-scale brain systems in ADHD: Beyond the prefrontal-striatal model. *Trends in Cognitive Sciences*, *16*, 17–26. https://doi.org/10.1016/j.tics.2011.11.007

Cebolla, A. M., Palmero-Soler, E., Dan, B., & Cheron, G. (2011). Frontal phasic and oscillatory generators of the N30 somatosensory evoked potential. *NeuroImage*, *54*, 1297–1306. https://doi.org/10.1016/j.neuroimage.2010.08.060

Cebolla, A.-M., Palmero-Soler, E., Leroy, A., & Cheron, G. (2017). EEG spectral generators involved in motor imagery: A swLORETA study. *Frontiers in Psychology*, *8*, 2133. https://doi.org/10.3389/fpsyg.2017.02133

Cheron, G., Leroy, A., Palmero-Soler, E., De Saedeleer, C., Bengoetxea, A., Cebolla, A.-M., Vidal, M., Dan, B., Berthoz, A., & McIntyre, J. (2014). Gravity influences top-down signals in visual processing. *PLoS ONE*, *9*, e82371. https://doi.org/10.1371/journal.pone.0082371

Chmielewski, W., Bluschke, A., Bodmer, B., Wolff, N., Roessner, V., & Beste, C. (2019). Evidence for an altered architecture and a hierarchical modulation of inhibitory control processes in ADHD. *Developmental Cognitive Neuroscience*, *36*, 100623. https://doi.org/10.1016/j.dcn.2019.100623

Chmielewski, W. X., Tiedt, A., Bluschke, A., Dippel, G., Roessner, V., & Beste, C. (2018). Effects of multisensory stimuli on inhibitory control in adolescent ADHD: It is the content of information that matters. *NeuroImage Clinical*, *19*, 527–537. https://doi.org/10.1016/j.nicl.2018.05.019

Chronaki, G., Soltesz, F., Benikos, N., & Sonuga-Barke, E. J. S. (2017). An electrophysiological investigation of reinforcement effects in attention deficit/hyperactivity disorder: Dissociating cue sensitivity from down-stream effects on target engagement and performance. *Developmental Cognitive Neuroscience*, *28*, 12–20. https://doi.org/10.1016/j.dcn.2017.10.003

Coghill, D. R., Seth, S., & Matthews, K. (2014). A comprehensive assessment of memory, delay aversion, timing, inhibition, decision making and variability in attention deficit hyperactivity disorder: Advancing beyond the three-pathway models. *Psychological Medicine*, *44*, 1989–2001. https://doi.org/10.1017/S0033291713002547

Coghill, D. R., Seth, S., Pedroso, S., Usala, T., Currie, J., & Gagliano, A. (2014). Effects of methylphenidate on cognitive functions in children and adolescents with attention-deficit/hyperactivity disorder: Evidence from a systematic review and a meta-analysis. *Biological Psychiatry*, *76*, 603–615.

Collins, D. L., Neelin, P., Peters, T. M., & Evans, A. C. (1994). Automatic 3D intersubject registration of MR volumetric data in standardized Talairach space. *Journal of Computer Assisted Tomography*, *18*, 192–205. https://doi.org/10.1097/00004728-199403000-00005

Danckaerts, M., Sonuga-Barke, E. J. S., Banaschewski, T., Buitelaar, J., Döpfner, M., Hollis, C., Santosh, P., Rothenberger, A., Sergeant, J., Steinhausen, H.-C., Taylor, E., Zuddas, A., & Coghill, D. (2010). The quality of life of children with attention deficit/hyperactivity disorder: A systematic review. *European Child and Adolescent Psychiatry*, *19*, 83–105. https://doi.org/10.1007/s00787-009-0046-3

DeFrance, J. F., Smith, S., Schweitzer, F. C., Ginsberg, L., & Sands, S. (1996). Topographical analyses of attention disorders of childhood. *International Journal of Neuroscience*, *87*, 41–61.

Delorme, A., & Makeig, S. (2004). EEGLAB: An open source toolbox for analysis of single-trial EEG dynamics including independent component analysis. *Journal of Neuroscience Methods*, *134*, 9–21.

Doehnert, M., Brandeis, D., Imhof, K., Drechsler, R., & Steinhausen, H.-C. (2010). Mapping attention-deficit/hyperactivity disorder from childhood to adolescence–no neurophysiologic evidence for a developmental lag of attention but some for inhibition. *Biological Psychiatry*, *67*, 608–616.

Donner, T. H., Kettermann, A., Diesch, E., Ostendorf, F., Villringer, A., & Brandt, S. A. (2002). Visual feature and conjunction searches of equal difficulty engage only partially overlapping frontoparietal networks. *NeuroImage*, *15*, 16–25. https://doi.org/10.1006/nimg.2001.0951

DuPaul, G. J., Anastopoulos, A. D., Power, T. J., Reid, R., Ikeda, M. J., & McGoey, K. E. (1998). Parent ratings of attention-deficit/hyperactivity disorder symptoms: Factor structure and normative data. *Journal of Psychopathology and Behavioral Assessment*, *20*, 83–102.

Engel, A. K., & Fries, P. (2010). Beta-band oscillations–signalling the status quo? *Current Opinion in Neurobiology*, *20*, 156–165.

Evans, A. C., Collins, D. L., Mills, S. R., Brown, E. D., Kelly, R. L., & Peters, T. M. (1993). 3D statistical neuroanatomical models from 305 MRI volumes. In *Presented at the 1993 IEEE conference record nuclear science symposium and medical imaging conference* (pp. 1813–1817), IEEE, San Francisco, CA, USA.

Faghiri, A., Stephen, J. M., Wang, Y.-P., Wilson, T. W., & Calhoun, V. D. (2018). Changing brain connectivity dynamics: From early childhood to adulthood. *Human Brain Mapping*, *39*, 1108–1117. https://doi.org/10.1002/hbm.23896

Faul, F., Erdfelder, E., Buchner, A., & Lang, A.-G. (2009). Statistical power analyses using G*Power 3.1: Tests for correlation and regression analyses. *Behavior Research Methods*, *41*, 1149–1160. https://doi.org/10.3758/BRM.41.4.1149

Fenollar-Cortés, J., Gallego-Martínez, A., & Fuentes, L. J. (2017). The role of inattention and hyperactivity/impulsivity in the fine motor coordination in children with ADHD. *Research in Developmental Disabilities*, *69*, 77–84. https://doi.org/10.1016/j.ridd.2017.08.003

Fontenelle, L. F., & Mendlowicz, M. V. (2008). The Wernicke-Kleist-Leonhard "short-circuiting": A missing link between attention deficit hyperactivity disorder, Tourette syndrome, and obsessive-compulsive disorder? *Medical Hypotheses*, *71*, 418–425. https://doi.org/10.1016/j.mehy.2008.03.043

Fox, M. D., Snyder, A. Z., Vincent, J. L., Corbetta, M., Van Essen, D. C., & Raichle, M. E. (2005). The human brain is intrinsically organized into dynamic, anticorrelated functional networks. *Proceedings of the National Academy of Sciences of the United States of America*, *102*, 9673–9678.

Gaffrey, M. S., Tillman, R., Barch, D. M., & Luby, J. L. (2018). Continuity and stability of preschool depression from childhood through adolescence and following the onset of puberty. *Comprehensive Psychiatry*, *86*, 39–46. https://doi.org/10.1016/j.comppsych.2018.07.010

Geselowitz, D. B. (1967). On bioelectric potentials in an inhomogeneous volume conductor. *Biophysical Journal*, *7*, 1–11.

Greven, C. U., Bralten, J., Mennes, M., O'Dwyer, L., van Hulzen, K. J. E., Rommelse, N., Schweren, L. J. S., Hoekstra, P. J., Hartman, C. A., Heslenfeld, D., Oosterlaan, J., Faraone, S. V., Franke, B., Zwiers, M. P., Arias-Vasquez, A., & Buitelaar, J. K. (2015). Developmentally stable whole-brain volume reductions and developmentally sensitive caudate and putamen volume alterations in those with attention-deficit/hyperactivity disorder and their unaffected siblings. *JAMA Psychiatry*, *72*, 490–499.

Holmes, A. P., Blair, R. C., Watson, J. D., & Ford, I. (1996). Nonparametric analysis of statistic images from functional mapping experiments. *Journal of Cerebral Blood Flow and Metabolism*, *16*, 7–22.

Hoogman, M., Bralten, J., Hibar, D. P., Mennes, M., Zwiers, M. P., Schweren, L. S. J., van Hulzen, K. J. E., Medland, S. E., Shumskaya, E., Jahanshad, N., de Zeeuw, P., Szekely, E., Sudre, G., Wolfers, T., Onnink, A. M. H., Dammers, J. T., Mostert, J. C., Vives-Gilabert, Y., Kohls, G., … Franke, B. (2017). Subcortical brain volume differences in participants with attention deficit hyperactivity disorder in children and adults: A cross-sectional mega-analysis. *The Lancet. Psychiatry*, *4*, 310–319.

Hoogman, M., Muetzel, R., Guimaraes, J. P., Shumskaya, E., Mennes, M., Zwiers, M. P., Jahanshad, N., Sudre, G., Wolfers, T., Earl, E. A., Soliva Vila, J. C., Vives-Gilabert, Y., Khadka, S., Novotny, S. E., Hartman, C. A., Heslenfeld, D. J., Schweren, L. J. S., Ambrosino, S., Oranje, B., … Franke, B. (2019). Brain imaging of the cortex in ADHD: A coordinated analysis of large-scale clinical and population-based samples. *American Journal of Psychiatry*, *176*, 531–542.

Janssen, T. W. P., Geladé, K., van Mourik, R., Maras, A., & Oosterlaan, J. (2016). An ERP source imaging study of the oddball task in children with Attention Deficit/Hyperactivity Disorder. *Clinical Neurophysiology*, *127*, 1351–1357.

Jensen, O., Goel, P., Kopell, N., Pohja, M., Hari, R., & Ermentrout, B. (2005). On the human sensorimotor-cortex beta rhythm: Sources and modeling. *NeuroImage*, *26*, 347–355.

Johnstone, S. J., Barry, R. J., & Clarke, A. R. (2013). Ten years on: A follow-up review of ERP research in attention-deficit/hyperactivity disorder. *Clinical Neurophysiology*, *124*, 644–657.

Jonkman, L. M., Kemner, C., Verbaten, M. N., Koelega, H. S., Camfferman, G., Gaag, R. J., Buitelaar, J. K., & van Engeland, H. (1997). Event-related potentials and performance of attention-deficit hyperactivity disorder: Children and normal controls in auditory and visual selective attention tasks. *Biological Psychiatry*, *41*, 595–611.

Jonkman, L. M., Kenemans, J. L., Kemner, C., Verbaten, M. N., & van Engeland, H. (2004). Dipole source localization of event-related brain activity indicative of an early visual selective attention deficit in ADHD children. *Clinical Neurophysiology*, *115*, 1537–1549.

Kaufman, J., Birmaher, B., Brent, D., Rao, U., Flynn, C., Moreci, P., Williamson, D., & Ryan, N. (1997). Schedule for affective disorders and schizophrenia for school-age children-present and lifetime version (K-SADS-PL): Initial reliability and validity data. *Journal of the American Academy of Child and Adolescent Psychiatry*, *36*, 980–988.

Kemner, C., Verbaten, M. N., Koelega, H. S., Buitelaar, J. K., van der Gaag, R. J., Camfferman, G., & van Engeland, H. (1996). Event-related brain potentials in children with attention-deficit and hyperactivity disorder: Effects of stimulus deviancy and task relevance in the visual and auditory modality. *Biological Psychiatry*, *40*, 522–534.

Khoshnoud, S., Shamsi, M., Nazari, M. A., & Makeig, S. (2018). Different cortical source activation patterns in children with attention deficit hyperactivity disorder during a time reproduction task. *Journal of Clinical and Experimental Neuropsychology*, *40*, 633–649. https://doi.org/10.1080/13803395.2017.1406897

Kilavik, B. E., Zaepffel, M., Brovelli, A., MacKay, W. A., & Riehle, A. (2013). The ups and downs of β oscillations in sensorimotor cortex. *Experimental Neurology*, *245*, 15–26.

Kim, J. W., Lee, J., Kim, H.-J., Lee, Y. S., & Min, K. J. (2015). Relationship between theta-phase gamma-amplitude coupling and attention-deficit/hyperactivity behavior in children. *Neuroscience Letters*, *590*, 12–17.

Klorman, R., Salzman, L. F., Pass, H. L., Borgstedt, A. D., & Dainer, K. B. (1979). Effects of methylphenidate on hyperactive children's evoked responses during passive and active attention. *Psychophysiology*, *16*, 23–29. https://doi.org/10.1111/j.1469-8986.1979.tb01432.x

Krauel, K., Duzel, E., Hinrichs, H., Lenz, D., Herrmann, C. S., Santel, S., Rellum, T., & Baving, L. (2009). Electrophysiological correlates of semantic processing during encoding of neutral and emotional pictures in patients with ADHD. *Neuropsychologia*, *47*, 1873–1882. https://doi.org/10.1016/j.neuropsychologia.2009.02.030

Kucyi, A., Hove, M. J., Biederman, J., Van Dijk, K. R. A., & Valera, E. M. (2015). Disrupted functional connectivity of cerebellar default network areas in attention-deficit/hyperactivity disorder. *Human Brain Mapping*, *36*, 3373–3386. https://doi.org/10.1002/hbm.22850

Lancaster, J. L., Woldorff, M. G., Parsons, L. M., Liotti, M., Freitas, C. S., Rainey, L., Kochunov, P. V., Nickerson, D., Mikiten, S. A., & Fox, P. T. (2000). Automated Talairach atlas labels for functional brain mapping. *Human Brain Mapping*, *10*, 120–131. https://doi.org/10.1002/1097-0193(200007)10:3<120:AID-HBM30>3.0.CO;2-8

Lawrence, C. A., Barry, R. J., Clarke, A. R., Johnstone, S. J., McCarthy, R., Selikowitz, M., & Broyd, S. J. (2005). Methylphenidate effects in attention deficit/hyperactivity disorder: Electrodermal and ERP measures during a continuous performance task. *Psychopharmacology (Berl.)*, *183*, 81–91. https://doi.org/10.1007/s00213-005-0144-y

Leech, R., & Sharp, D. J. (2014). The role of the posterior cingulate cortex in cognition and disease. *Brain*, *137*, 12–32. https://doi.org/10.1093/brain/awt162

Lenartowicz, A., Delorme, A., Walshaw, P. D., Cho, A. L., Bilder, R. M., McGough, J. J., McCracken, J. T., Makeig, S., & Loo, S. K. (2014). Electroencephalography correlates of spatial working memory deficits in attention-deficit/hyperactivity disorder: Vigilance, encoding, and maintenance. *Journal of Neuroscience*, *34*, 1171–1182. https://doi.org/10.1523/JNEUROSCI.1765-13.2014

Lenartowicz, A., & Loo, S. K. (2014). Use of EEG to diagnose ADHD. *Current Psychiatry Reports*, *16*, 498. https://doi.org/10.1007/s11920-014-0498-0

Lenartowicz, A., Lu, S., Rodriguez, C., Lau, E. P., Walshaw, P. D., McCracken, J. T., Cohen, M. S., & Loo, S. K. (2016). Alpha desynchronization and fronto-parietal connectivity during spatial working memory encoding deficits in ADHD: A simultaneous EEG-fMRI study. *NeuroImage Clinical*, *11*, 210–223. https://doi.org/10.1016/j.nicl.2016.01.023

Lenartowicz, A., Truong, H., Salgari, G. C., Bilder, R. M., McGough, J., McCracken, J. T., & Loo, S. K. (2019). Alpha modulation during working memory encoding predicts neurocognitive impairment in ADHD. *Journal of Child Psychology and Psychiatry*. *60*, 917–926.

Lenz, D., Krauel, K., Flechtner, H.-H., Schadow, J., Hinrichs, H., & Herrmann, C. S. (2010). Altered evoked gamma-band responses reveal impaired early visual processing in ADHD children.

Neuropsychologia, *48*, 1985–1993. https://doi.org/10.1016/j.neuropsychologia.2010.03.019

Lenz, D., Krauel, K., Schadow, J., Baving, L., Duzel, E., & Herrmann, C. S. (2008). Enhanced gamma-band activity in ADHD patients lacks correlation with memory performance found in healthy children. *Brain Research*, *1235*, 117–132.

Leroy, A., Cevallos, C., Cebolla, A.-M., Caharel, S., Dan, B., & Cheron, G. (2017). Short-term EEG dynamics and neural generators evoked by navigational images. *PLoS ONE*, *12*, e0178817. https://doi.org/10.1371/journal.pone.0178817

Leroy, A., Petit, G., Zarka, D., Cebolla, A. M., Palmero-Soler, E., Strul, J., Dan, B., Verbanck, P., & Cheron, G. (2018). EEG dynamics and neural generators in implicit navigational image processing in adults with ADHD. *Neuroscience*, *373*, 92–105. https://doi.org/10.1016/j.neuroscience.2018.01.022

Lin, F.-H., Witzel, T., Hämäläinen, M. S., Dale, A. M., Belliveau, J. W., & Stufflebeam, S. M. (2004). Spectral spatiotemporal imaging of cortical oscillations and interactions in the human brain. *NeuroImage*, *23*, 582–595. https://doi.org/10.1016/j.neuroimage.2004.04.027

Lindquist, M. A., & Mejia, A. (2015). Zen and the art of multiple comparisons. *Psychosomatic Medicine*, *77*, 114–125. https://doi.org/10.1097/PSY.0000000000000148

López, V., López-Calderón, J., Ortega, R., Kreither, J., Carrasco, X., Rothhammer, P., Rothhammer, F., Rosas, R., & Aboitiz, F. (2006). Attention-deficit hyperactivity disorder involves differential cortical processing in a visual spatial attention paradigm. *Clinical Neurophysiology*, *117*, 2540–2548. https://doi.org/10.1016/j.clinph.2006.07.313

Michael, R. L., Klorman, R., Salzman, L. F., Borgstedt, A. D., & Dainer, K. B. (1981). Normalizing effects of methylphenidate on hyperactive children's vigilance performance and evoked potentials. *Psychophysiology*, *18*, 665–677. https://doi.org/10.1111/j.1469-8986.1981.tb01841.x

Mohl, B., Ofen, N., Jones, L. L., Robin, A. L., Rosenberg, D. R., Diwadkar, V. A., Casey, J. E., & Stanley, J. A. (2015). Neural dysfunction in ADHD with reading disability during a word rhyming continuous performance task. *Brain and Cognition*, *99*, 1–7. https://doi.org/10.1016/j.bandc.2015.04.009

Nakao, T., Radua, J., Rubia, K., & Mataix-Cols, D. (2011). Gray matter volume abnormalities in ADHD: Voxel-based meta-analysis exploring the effects of age and stimulant medication. *American Journal of Psychiatry*, *168*, 1154–1163. https://doi.org/10.1176/appi.ajp.2011.11020281

Nichols, T. E., & Holmes, A. P. (2002). Nonparametric permutation tests for functional neuroimaging: A primer with examples. *Human Brain Mapping*, *15*, 1–25. https://doi.org/10.1002/hbm.1058

O'Neill, S., Rajendran, K., Mahbubani, S. M., & Halperin, J. M. (2017). Preschool predictors of ADHD symptoms and impairment during childhood and adolescence. *Current Psychiatry Reports*, *19*, 95. https://doi.org/10.1007/s11920-017-0853-z

Overtoom, C. C., Verbaten, M. N., Kemner, C., Kenemans, J. L., van Engeland, H., Buitelaar, J. K., Camfferman, G., & Koelega, H. S. (1998). Associations between event-related potentials and measures of attention and inhibition in the Continuous Performance Task in children with ADHD and normal controls. *Journal of the American Academy of Child and Adolescent Psychiatry*, *37*, 977–985. https://doi.org/10.1097/00004583-199809000-00018

Palmero-Soler, E., Dolan, K., Hadamschek, V., & Tass, P. A. (2007). swLORETA: A novel approach to robust source localization and synchronization tomography. *Physics in Medicine & Biology*, *52*, 1783–1800. https://doi.org/10.1088/0031-9155/52/7/002

Pardo, J. V., Pardo, P. J., Janer, K. W., & Raichle, M. E. (1990). The anterior cingulate cortex mediates processing selection in the Stroop attentional conflict paradigm. *Proceedings of the National Academy of Sciences of the United States of America*, *87*, 256–259. https://doi.org/10.1073/pnas.87.1.256

Pascual-Marqui, R. D. (2002). Standardized low-resolution brain electromagnetic tomography (sLORETA): Technical details. *Methods and Findings in Experimental and Clinical Pharmacology*, *24*(Suppl D), 5–12.

Pascual-Marqui, R. D., Esslen, M., Kochi, K., & Lehmann, D. (2002). Functional imaging with low-resolution brain electromagnetic tomography (LORETA): A review. *Methods and Findings in Experimental and Clinical Pharmacology*, *24*(Suppl C), 91–95.

Perchet, C., Revol, O., Fourneret, P., Mauguière, F., & Garcia-Larrea, L. (2001). Attention shifts and anticipatory mechanisms in hyperactive children: An ERP study using the Posner paradigm. *Biological Psychiatry*, *50*, 44–57.

Pfurtscheller, G., & Neuper, C. (1994). Event-related synchronization of mu rhythm in the EEG over the cortical hand area in man. *Neuroscience Letters*, *174*, 93–96.

Polanczyk, G. V., Salum, G. A., Sugaya, L. S., Caye, A., & Rohde, L. A. (2015). Annual research review: A meta-analysis of the worldwide prevalence of mental disorders in children and adolescents. *Journal of Child Psychology and Psychiatry*, *56*, 345–365. https://doi.org/10.1111/jcpp.12381

Robaey, P., Breton, F., Dugas, M., & Renault, B. (1992). An event-related potential study of controlled and automatic processes in 6-8-year-old boys with attention deficit hyperactivity disorder. *Electroencephalography and Clinical Neurophysiology*, *82*, 330–340. https://doi.org/10.1016/0013-4694(92)90003-Z

Rubia, K., Halari, R., Cubillo, A., Mohammad, A.-M., Brammer, M., & Taylor, E. (2009). Methylphenidate normalises activation and functional connectivity deficits in attention and motivation networks in medication-naïve children with ADHD during a rewarded continuous performance task. *Neuropharmacology*, *57*, 640–652. https://doi.org/10.1016/j.neuropharm.2009.08.013

Saad, J. F., Griffiths, K. R., Kohn, M. R., Clarke, S., Williams, L. M., & Korgaonkar, M. S. (2017). Regional brain network organization distinguishes the combined and inattentive subtypes of Attention Deficit Hyperactivity Disorder. *NeuroImage Clinical*, *15*, 383–390. https://doi.org/10.1016/j.nicl.2017.05.016

Satterfield, J. H., Schell, A. M., & Nicholas, T. (1994). Preferential neural processing of attended stimuli in attention-deficit hyperactivity disorder and normal boys. *Psychophysiology*, *31*, 1–10. https://doi.org/10.1111/j.1469-8986.1994.tb01018.x

Segal, D., Mashal, N., & Shalev, L. (2015). Semantic conflicts are resolved differently by adults with and without ADHD. *Research in Developmental Disabilities*, *47*, 416–429. https://doi.org/10.1016/j.ridd.2015.09.024

Senderecka, M., Grabowska, A., Gerc, K., Szewczyk, J., & Chmylak, R. (2012). Event-related potentials in children with attention deficit hyperactivity disorder: An investigation using an auditory oddball task. *International Journal of Psychophysiology*, *85*, 106–115. https://doi.org/10.1016/j.ijpsycho.2011.05.006

Smith, J. L., Johnstone, S. J., & Barry, R. J. (2004). Inhibitory processing during the Go/NoGo task: An ERP analysis of children with attention-deficit/hyperactivity disorder. *Clinical Neurophysiology*, *115*, 1320–1331. https://doi.org/10.1016/j.clinph.2003.12.027

Spronk, M., Jonkman, L. M., & Kemner, C. (2008). Response inhibition and attention processing in 5- to 7-year-old children with and without symptoms of ADHD: An ERP study. *Clinical Neurophysiology*, *119*, 2738–2752. https://doi.org/10.1016/j.clinph.2008.09.010

Steger, J., Imhof, K., Steinhausen, H., & Brandeis, D. (2000). Brain mapping of bilateral interactions in attention deficit hyperactivity disorder and control boys. *Clinical Neurophysiology*, *111*, 1141–1156. https://doi.org/10.1016/S1388-2457(00)00311-4

Stoodley, C. J. (2016). The cerebellum and neurodevelopmental disorders. *Cerebellum*, *15*, 34–37. https://doi.org/10.1007/s12311-015-0715-3

Strandburg, R. J., Marsh, J. T., Brown, W. S., Asarnow, R. F., Higa, J., Harper, R., & Guthrie, D. (1996). Continuous-processing–related event-related potentials in children with attention deficit hyperactivity disorder. *Biological Psychiatry*, *40*, 964–980.

Tal, I., & Abeles, M. (2016). Temporal accuracy of human cortico-cortical interactions. *Journal of Neurophysiology*, *115*, 1810–1820.

van der Stelt, O., van der Molen, M., Boudewijn Gunning, W., & Kok, A. (2001). Neuroelectrical signs of selective attention to color in boys with attention-deficit hyperactivity disorder. *Brain Research Cognitive Brain Research*, *12*, 245–264. https://doi.org/10.1016/S0926-6410(01)00055-6

van Mourik, R., Oosterlaan, J., Heslenfeld, D. J., Konig, C. E., & Sergeant, J. A. (2007). When distraction is not distracting: A behavioral and ERP study on distraction in ADHD. *Clinical Neurophysiology*, *118*, 1855–1865. https://doi.org/10.1016/j.clinph.2007.05.007

Voelkl, B., Altman, N. S., Forsman, A., Forstmeier, W., Gurevitch, J., Jaric, I., Karp, N. A., Kas, M. J., Schielzeth, H., Van de Casteele, T., & Würbel, H. (2020). Reproducibility of animal research in light of biological variation. *Nature Reviews Neuroscience*, *21*, 384–393. https://doi.org/10.1038/s41583-020-0313-3

Wagner, M., Fuchs, M., & Kastner, J. (2004). Evaluation of sLORETA in the presence of noise and multiple sources. *Brain Topography*, *16*, 277–280. https://doi.org/10.1023/B:BRAT.0000032865.58382.62

Yorbik, O., Ozdag, M. F., Olgun, A., Senol, M. G., Bek, S., & Akman, S. (2008). Potential effects of zinc on information processing in boys with attention deficit hyperactivity disorder. *Progress in Neuro-Psychopharmacology and Biological Psychiatry*, *32*, 662–667.

Yordanova, J., Heinrich, H., Kolev, V., & Rothenberger, A. (2006). Increased event-related theta activity as a psychophysiological marker of comorbidity in children with tics and attention-deficit/hyperactivity disorders. *NeuroImage*, *32*, 940–955. https://doi.org/10.1016/j.neuroimage.2006.03.056

Yordanova, J., Kolev, V., & Rothenberger, A. (2013). Event-related oscillations reflect functional asymmetry in children with attention deficit/hyperactivity disorder. *Supplements to Clinical Neurophysiology*, *62*, 289–301.

Zammit, N., Falzon, O., Camilleri, K., & Muscat, R. (2018). Working memory alpha–beta band oscillatory signatures in adolescents and young adults. *European Journal of Neuroscience*, *48*, 2527–2536.

How to cite this article: Zarka D, Leroy A, Cebolla A, Cevallos C, Palmero-Soler E, Cheron G. Neural generators involved in visual cue processing in children with attention-deficit/hyperactivity disorder (ADHD). *Eur J Neurosci*. 2020;00:1–18. https://doi.org/10.1111/ejn.15040